Progress In Electromagnetics Research, Vol. 110, 23–42, 2010

HYBRID FINITE-DIFFERENCE/MODE-MATCHING METHOD FOR ANALYSIS OF SCATTERING FROM ARBITRARY CONFIGURATION OF ROTATIONALLY-SYMMETRICAL POSTS

A. Kusiek and J. Mazur

Faculty of Electronics, Telecommunications and Informatics
Department of Microwave and Antenna Engineering
Gdansk University of Technology
11/12 Gabriela Narutowicza Street, 80-233 Gdansk, Poland

Abstract—In this paper, the hybrid approach to the analysis of electromagnetic wave scattering from arbitrary configuration of body-of-revolution (BOR) posts is presented. The proposed approach is based on the representation of each scatterer or set of scatterers by an effective sphere with the known boundary conditions defined by transmission matrix. In the analysis of each single axially-symmetrical post with irregular shape we utilize the finite-difference frequency-domain/mode-matching technique (FDFD/MM). Then the scattering parameters of investigated set of posts are obtained utilizing the analytical iterative scattering procedure (ISP). This work is an extension of our previously published results where the proposed technique was defined in cylindrical coordinates and was limited to configurations of infinitely long parallel cylinders with arbitrary cross-section. In this paper we extend this method by formulating it in spherical coordinates. This allows us to significantly increase the versatility of the developed approach and in result to include in the analysis the sets of arbitrary located and oriented rotationally-symmetrical posts. The accuracy and efficiency of the proposed technique are discussed. The presented numerical results are verified with the ones obtained from commercial software.

Received 24 September 2010, Accepted 18 October 2010, Scheduled 6 November 2010
Corresponding author: Adam Kusiek (adakus@eti.pg.gda.pl).

1. INTRODUCTION

The analysis of scattering from an arbitrary set of body-of-revolution (BOR) objects is crucial in many recent civil and military applications (e.g., antenna systems for wireless communication [1, 2] or objects identification in radar systems [3–5]). This creates the demand for highly efficient and accurate analysis techniques of this phenomenon. The numerical efficiency of the developed algorithms can be improved by exploiting symmetry properties of the objects in the considered structures. As a result, this allows to reduce the three dimensional (3D) problem to a two-and-a-half (2.5D) dimensional one which is less time consuming and involves lower requirements for computer resources.

Analysis techniques of BOR objects have been developed intensively in literature for a long time [6–16]. Initially, the method-of-moments (MoM) was used to solve the problem of axially-symmetrical perfectly conducting post [6]. This approach was extended by many other researchers to the analysis of radiating and scattering problems from other kind of objects, e.g., homogenous dielectrics [7], dielectric coated conductors [8], lossy dielectrics [9] inhomogeneous dielectrics [10] or elongated dielectric cylinders [15, 16]. The drawback of this approach is its rapidly increasing complexity for the inhomogeneous structures. Hence, this technique is limited to the small group of homogenous or piecewise homogenous objects.

In the analysis of inhomogeneous BOR objects with complex geometry the more numerically powerful techniques are hybrid methods [11–14] which combine the partially-differential equation (PDE) based methods (e.g., finite-difference time-domain (FDTD) method, finite element method (FEM)) with analytical ones (e.g., Mode Matching (MM) technique, MoM). In these techniques the discrete approach (FDTD, FEM) is only used in the limited area surrounding the post, where the analytical solution of the problem is difficult to determine. In the outer homogenous region the continuous analytical form of the fields is assumed. The advantage of this approach is that the complexity of the problem can be reduced, and time and memory efficiency algorithms can be achieved. In the literature one can find different hybrid techniques, which allow to solve the problem of scattering with different accuracy and efficiency [11, 12, 14]. In [11] the investigated rotationally symmetrical post was enclosed in an artificial spherical object. In the inner region FEM technique was used and the solution was combined with the exterior fields defined by series of eigenfunctions. This technique became inefficient in the case of long objects. To overcame this problem the FDTD-PML technique was proposed in [12] where the cylindrical discrete region was used, which

is more suitable for elongated BORs. However, due to the artificial reflections in PML, the discrete area have to be increased which results in decreasing the efficiency of this approach. In [14] the FE-BI technique was proposed to the analysis of arbitrary inhomogeneous objects. In this technique MoM was used to analyze the fields in exterior area and as a result the mesh truncation could be placed very close to the object to minimize memory usage.

All the mentioned hybrid techniques [11, 12, 14] are limited to the single object analysis. In order to consider the arbitrary set of objects in this paper we propose the hybrid approach which is based on the combination of finite-difference frequency-domain/mode matching (FDFD/MM) technique with the analytical iterative scattering procedure (ISP) [17]. In our approach each scatterer or set of scatterers is treated as an effective sphere which encloses investigated elements and is represented by transmission matrix defining the relation between the incident and scattered fields. In the case of single post with irregular shape the transmission matrix $\mathbf{T}$ is evaluated with the use of combination of finite-difference and mode-matching technique. Since the $\mathbf{T}$-matrix of each post is known we utilize the defined in spherical coordinates ISP to determine the total transmission matrix ($\mathbf{T}_{total}$-matrix) of arbitrary configuration of objects. Transmission matrix depends on the geometry and material properties of the structure and does not depend on the excitation. Hence, it can be easily applied to the analysis of scattering from the configurations of objects illuminated with arbitrary incident field. This paper is an extension of our previously published work. In [18] the proposed technique defined in cylindrical coordinates was successfully applied to the analysis of the sets of parallel cylinders with arbitrary cross-section. In this paper we formulate the method in spherical coordinates what significantly improves the versatility of this approach in comparison to [18]. As a result configurations of arbitrary located and rotated objects of finite height can be included in the analysis. The convergence and accuracy of the method are verified and discussed. The presented results are compared with the ones obtained from commercial software QuickWave 3D (FDTD) [19].

2. FORMULATION OF THE PROBLEM

In the analysis of multiple element configuration with the use of proposed hybrid approach we can distinguish two main stages (see Fig. 1). The first one considers analyzing each individual post in its local coordinate system. It involves defining an artificial homogeneous spherical object enclosing considered post. In this stage we use

the FDFD/MM technique to calculate the transmission matrix **T** of each single element, which defines the relation between incident and scattered fields. In the second stage the multiple post configuration is analyzed with the use of the analytical iterative scattering procedure (ISP). In the analysis we again define the artificial spherical object enclosing the whole set. The result of this approach is a total transmission matrix $\mathbf{T}_{total}$.

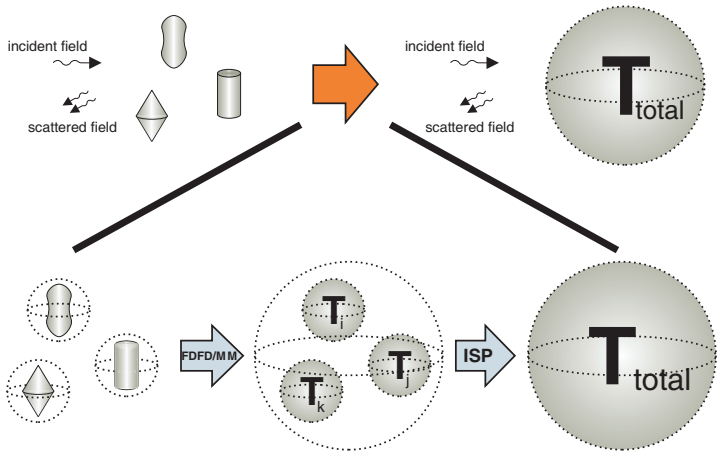

Figure 1. Scheme of the analysis of arbitrary configuration of objects using hybrid FDFD/MM method.

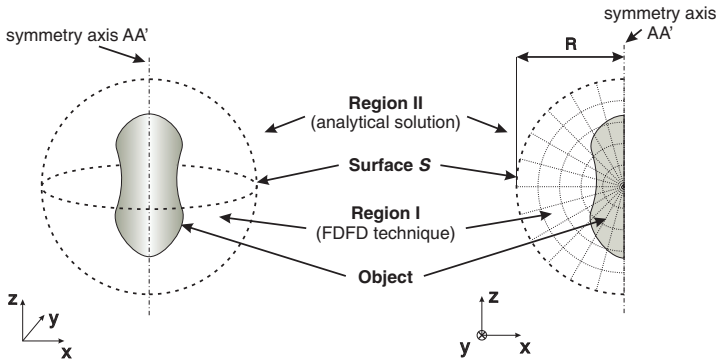

Figure 2. Single axially-symmetrical object in local coordinates.

2.1. Single Object

We start our analysis from a single object in its local coordinate system (see Fig. 2). In our approach we introduce lateral surface $\mathcal{S}$:

$$S : \begin{cases} r & = & R, \\ \theta & \in & [0, \pi], \\ \varphi & \in & [0, 2\pi]. \end{cases} \tag{1}$$

which surrounds analyzed object and divides the computational domain into two regions, where the analytical (region II) and discrete FDFD (region I) solutions of Maxwell equations are used, respectively. The aim of the analysis is to determine the relation between incident and scattered fields in region II which is defined by transmission matrix **T**. Such relation can be simply found for any spherical object with the boundary conditions defined by impedance matrix **Z** relating electric and magnetic fields (see Section 2.1.1). Since, our object has irregular cross-section we use FDFD technique to determine the **Z** matrix on the artificial spherical surface $\mathcal{S}$ (see Section 2.1.2). In result we can treat investigated scatterer as an effective sphere with the known boundary conditions defined by **Z**-matrix. Finally, utilizing mode-matching technique we are obtaining the **T**-matrix of the considered element.

*2.1.1. **T**-matrix*

In region II the total tangential to the surface $\mathcal{S}$ components of electric and magnetic fields are expressed as follows:

$$\begin{aligned} \mathbf{E}_t^{II} = & \sum_{i=1}^{2} \sum_{n=1}^{N} \sum_{m=-n}^{n} \left\{ A_{inm}^{E} z_n^i(k_0 r) \mathbf{M}_{nm}^t(\theta, \varphi) \right. \\ & \left. + A_{inm}^{H} \frac{1}{k_0 r} \frac{\partial (r z_n^i(k_0 r))}{\partial r} \mathbf{N}_{nm}^t(\theta, \varphi) \right\}, \end{aligned} \tag{2}$$

$$\begin{aligned} \mathbf{H}_t^{II} = & -\frac{k_0}{j\omega\mu_0} \sum_{i=1}^{2} \sum_{n=1}^{N} \sum_{m=-n}^{n} \left\{ A_{inm}^{E} \frac{1}{k_0 r} \frac{\partial (r z_n^i(k_0 r))}{\partial r} \mathbf{N}_{nm}^t(\theta, \varphi) \right. \\ & \left. + A_{inm}^{H} z_n^i(k_0 r) \mathbf{M}_{nm}^t(\theta, \varphi) \right\}, \end{aligned} \tag{3}$$

where $\omega = 2\pi f_0$, $k_0 = \omega\sqrt{\mu_0 \varepsilon_0}$, f_0 is the frequency of analysis, μ_0 and ε_0 are magnetic permeability and electric permittivity of free space, $z_n^1(\cdot)$ and $z_n^2(\cdot)$ denotes spherical Bessel and second kind Hankel functions of n-th order, $\mathbf{M}_{nm}^t(\cdot, \cdot)$ and $\mathbf{N}_{nm}^t(\cdot, \cdot)$ are vector functions

defined as follows:

$$\mathbf{M}^t_{nm}(\theta,\varphi) = e^{jm\varphi}\left\{\frac{jm}{\sin\theta}P^m_n(\cos\theta)\mathbf{i}_\theta - \frac{\partial P^m_n(\cos\theta)}{\partial\theta}\mathbf{i}_\varphi\right\}, \tag{4}$$

$$\mathbf{N}^t_{nm}(\theta,\varphi) = e^{jm\varphi}\left\{\frac{\partial P^m_n(\cos\theta)}{\partial\theta}\mathbf{i}_\theta + \frac{jm}{\sin\theta}P^m_n(\cos\theta)\mathbf{i}_\varphi\right\}, \tag{5}$$

and $P^m_n(\cdot)$ is an associated Legendre function defined according to [20]. In Equations (2) and (3) the field expansion coefficients can be related using transmission matrix as follows:

$$\mathbf{A}_2 = \mathbf{T}\mathbf{A}_1, \tag{6}$$

where $\mathbf{A}_1$ is a column vector of known incident field coefficients A_{1nm} (e.g., plane wave — see Section 2.3) and $\mathbf{A}_2$ is a column vector of the unknown coefficients A_{2nm} of scattered field.

In order to determine $\mathbf{T}$-matrix at first we define the tangential components of electric and magnetic fields on lateral surface $\mathcal{S}$ in region I:

$$\mathbf{E}^I_t(R,\theta,\varphi) = \sum_{n=1}^{N}\sum_{m=-n}^{n}\left\{C^E_{nm}\mathbf{M}^t_{nm}(\theta,\varphi) + C^H_{nm}\mathbf{N}^t_{nm}(\theta,\varphi)\right\}, \tag{7}$$

$$\mathbf{H}^I_t(R,\theta,\varphi) = -\frac{k_0}{j\omega\mu}\sum_{n=1}^{N}\sum_{m=-n}^{n}\left\{D^E_{nm}\mathbf{N}^t_{nm}(\theta,\varphi) + D^H_{nm}\mathbf{M}^t_{nm}(\theta,\varphi)\right\}, \tag{8}$$

where C^E_{nm}, C^H_{nm}, D^E_{nm} and D^H_{nm} are the unknown expansion field coefficients. Now, by imposing the boundary continuity conditions between tangential components of electric and magnetic fields on surface $\mathcal{S}$ the following set of equations is obtained:

$$\begin{aligned} E^{II}_t(R,\theta,\varphi) &= E^I_t(R,\theta,\varphi),\\ H^{II}_t(R,\theta,\varphi) &= H^I_t(R,\theta,\varphi), \end{aligned} \tag{9}$$

where $\theta \in [0,\pi]$, $\varphi \in [0,2\pi]$. Taking the advantage of orthogonality of $\mathbf{M}^t_{nm}(\cdot,\cdot)$ and $\mathbf{N}^t_{nm}(\cdot,\cdot)$ set of Equation (9) can be rewritten in the matrix form as follows:

$$\mathbf{M}^E_{A1}\mathbf{A}_1 + \mathbf{M}^E_{A2}\mathbf{A}_2 = \mathbf{C}, \tag{10}$$

$$\mathbf{M}^H_{A1}\mathbf{A}_1 + \mathbf{M}^H_{A2}\mathbf{A}_2 = \mathbf{D}, \tag{11}$$

where all matrices are defined in Appendix A. Now we can introduce the impedance $\mathbf{Z}$-matrix representation of the object:

$$\mathbf{C} = \mathbf{Z}\mathbf{D}, \tag{12}$$

which defines the relation between the expansion coefficients $\mathbf{C}$ and $\mathbf{D}$ of tangential electric (7) and magnetic (8) fields, respectively.

Substituting relation (12) to (10) and then after some algebra manipulations of obtained relation with (11) we can derive the following expression:

$$\mathbf{T} = \left(\mathbf{Z}\mathbf{M}_{A2}^{H} - \mathbf{M}_{A2}^{E}\right)^{-1}\left(\mathbf{M}_{A1}^{E} - \mathbf{Z}\mathbf{M}_{A1}^{H}\right). \tag{13}$$

Relation (13) allows us to determine **T**-matrix for any spherical object with the known boundary conditions defined by **Z**-matrix.

It must be emphasized that **T**-matrix depends on the geometry and material properties of the object but not on the excitation. This approach allows us to limit our consideration to region II where the scatterer is treated as an effective sphere described by its **T**-matrix. For such an effective sphere the scattered field can be found for any incident wave. Moreover, the advantage of this approach is that, the transmission matrix of arbitrary rotated object by any set of Euler angles α, β, γ [21] can be simply derived from the following analytical relation:

$$\mathbf{T}_{\alpha,\beta,\gamma} = \mathbf{D}^{-1}\mathbf{T}_0\mathbf{D}, \tag{14}$$

where

$$\mathbf{D} = \begin{bmatrix} \mathbf{D}_0 & \mathbf{0} & \cdots & \mathbf{0} \\ \mathbf{0} & \mathbf{D}_1 & \ddots & \vdots \\ \vdots & \ddots & \ddots & \mathbf{0} \\ \mathbf{0} & \cdots & \mathbf{0} & \mathbf{D}_N \end{bmatrix} \quad \text{and} \quad \mathbf{D}_n = \begin{bmatrix} D_{n(-n)}^{-n} & \cdots & D_{n(-n)}^{n} \\ \vdots & \ddots & \vdots \\ D_{nn}^{-n} & \cdots & D_{nn}^{n} \end{bmatrix}$$

and D_{mn}^{k} are the coefficients defined by recurrence relations presented in [22].

*2.1.2. **Z**-matrix*

Since the analyzed axially-symmetrical post has irregular shape the determination of its **Z** matrix representation with the usage of analytical techniques becomes difficult. In order to solve this problem we use 2.5D finite-difference frequency domain technique (FDFD). In our formulation we assume that the variation of field in φ-direction is described by a series of eigenfunctions $e^{jm\varphi}$ $(m = -M, \ldots, M)$. Utilizing orthogonality properties of these functions the above problem can be solved for each eigenvalue m separately. In this case Maxwell's

equations take the following form:

$$\begin{bmatrix} 0 & -\frac{jm}{r\sin\theta} & \frac{1}{r\sin\theta}\frac{\partial \sin\theta}{\partial\theta} \\ \frac{jm}{r\sin\theta} & 0 & -\frac{1}{r}\frac{\partial r}{\partial r} \\ -\frac{1}{r}\frac{\partial}{\partial\theta} & \frac{1}{r}\frac{\partial r}{\partial r} & 0 \end{bmatrix} \begin{bmatrix} E_r \\ E_\theta \\ E_\varphi \end{bmatrix} = -j\omega\mu_0\mu_r \begin{bmatrix} H_r \\ H_\theta \\ H_\varphi \end{bmatrix}, \quad (15)$$

$$\begin{bmatrix} 0 & -\frac{jm}{r\sin\theta} & \frac{1}{r\sin\theta}\frac{\partial \sin\theta}{\partial\theta} \\ \frac{jm}{r\sin\theta} & 0 & -\frac{1}{r}\frac{\partial r}{\partial r} \\ -\frac{1}{r}\frac{\partial}{\partial\theta} & \frac{1}{r}\frac{\partial r}{\partial r} & 0 \end{bmatrix} \begin{bmatrix} H_r \\ H_\theta \\ H_\varphi \end{bmatrix} = j\omega\varepsilon_0\varepsilon_r \begin{bmatrix} E_r \\ E_\theta \\ E_\varphi \end{bmatrix}. \quad (16)$$

Now we discretize the computational domain in $\varphi = \text{const}$ semi-plane with Yee-mesh defined in spherical coordinates (see Fig. 3). As a result Equations (15) and (16) can be rewritten in a discrete form as follows:

$$\mathbf{P}_1^m(\mathbf{Q}\mathbf{E}^m + \mathbf{Q}_b\mathbf{E}_b^m) = j\omega\mu_0\mu_r\mathbf{H}^m, \quad (17)$$

$$\mathbf{P}_2^m\mathbf{H}^m = j\omega\varepsilon_0\varepsilon_r\mathbf{E}^m, \quad (18)$$

where $\mathbf{P}_1$ and $\mathbf{P_2}$ are matrices of derivatives, $\mathbf{E}$ and $\mathbf{H}$ are the column vectors of electric and magnetic field component samples in interior area of the region I and $\mathbf{E}_b$ contains samples of tangential electric field components located at surface $\mathcal{S}$.

In order to solve the problem for any excitation $\mathbf{E}_b$ we have to also define the boundary conditions for field components E_r, E_φ and H_r at the axis of symmetry $AA' : \{r \in [0, R], \theta = \{0, \pi\}\}$. From Equations (17) and (18) it can be found that only E_r is used to found other probes of fields in area of discretization. In the case of $m = 0$ the value of E_r at axis AA' can be found from Ampere's law [23] and takes the following form:

$$E_{r(i,k)} = (-1)^{\alpha_k}\frac{H_{\varphi(i,k)}}{j\omega\varepsilon_0\varepsilon_{r(i,k)}r_{h(i)}\left(1-\cos\left(\Delta_\theta/2\right)\right)}, \quad (19)$$

In above relation $\varepsilon_{r(i,k)}$ is a dielectric constant in the r-direction for the cell containing $E_{r(i,k)}$, $i = 1, \ldots, I$, $k = \{1, K\}$ and

$$\alpha_k = \begin{cases} 0 & \text{dla} \quad k = 1, \\ 1 & \text{dla} \quad k = K. \end{cases} \quad (20)$$

In all the other cases ($|m| > 0$) the value of E_r at symmetry axis AA' is equal zero.

After some algebra manipulations of (17) and (18) we are obtaining the following relation:

$$\mathbf{H}^m = -j\omega\varepsilon_0(\mathbf{G}^m)^{-1}\mathbf{P}_1^m\mathbf{D}_1\mathbf{Q}_b\mathbf{E}_b^m, \quad (21)$$

where $\mathbf{G}^m$ takes the following form

$$\mathbf{G}^m = \mathbf{P}_1^m\mathbf{Q}\varepsilon_r^{-1}\mathbf{P}_2^m + \omega^2\mu_0\varepsilon_0\mathbf{I}_{(3W+1)\times(3W+1)}, \quad (22)$$

which allow us to determine the magnetic field $\mathbf{H}$ for assumed boundary electric field $\mathbf{E}_b$. In order to determine the impedance matrix $\mathbf{Z}_m$ we assume the following excitation of the structure:

$$\mathbf{E_b^m} = \begin{bmatrix} \mathbf{E}^m_{b(M_t)} & \mathbf{0} \\ \mathbf{0} & \mathbf{E}^m_{b(N_t)} \end{bmatrix}, \tag{23}$$

where:

$$\left[\mathbf{E}^m_{b(M_t)}\right]_{k,n} = C^E_{nm}\mathbf{M}^t_{nm}(\theta_{(k)}, \varphi), \tag{24}$$

$$\left[\mathbf{E}^m_{b(N_t)}\right]_{k,n} = C^H_{nm}\mathbf{N}^t_{nm}(\theta_{(k)}, \varphi) \tag{25}$$

for $n = m, \ldots, N$, $k = 1, \ldots, K$ and C^E_{nm}, C^H_{nm} are the arbitrary assumed coefficients. As a result of this excitation we are obtaining the column vector of magnetic field components $\mathbf{H}$ defined in the interior area of region I. Then utilizing Equation (18) we can also obtain the column vector of electric field components $\mathbf{E}$.

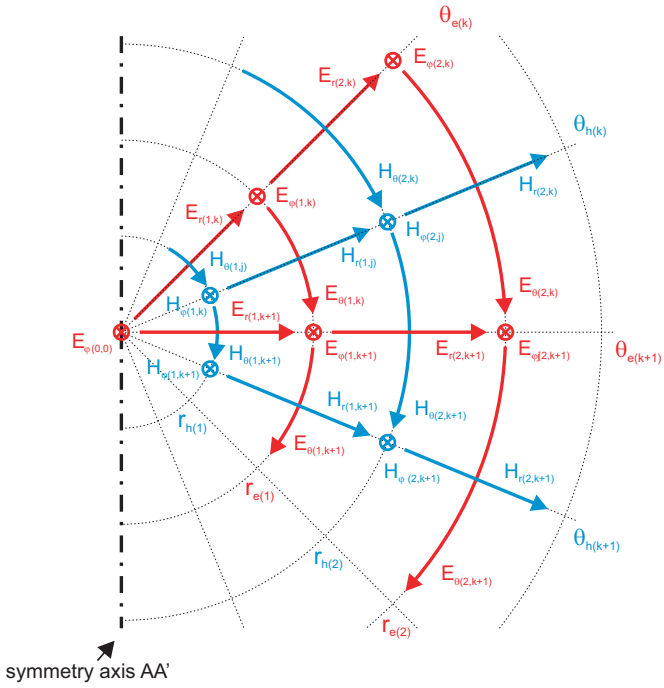

Figure 3. Yee-grid defined in spherical coordinates in φ-const semi-plane.

Now the tangential components of electric and magnetic fields defined at the surface $\mathcal{S}$ are expanded in the series which coefficients can be found from the following relations:

$$F_{nm}^{E} = \frac{1}{\epsilon_{nm}} \int_0^{2\pi} \int_0^{\pi} \mathbf{f}_{nm}(R,\theta,\varphi)\mathbf{M}_{nm}^{t}(\theta,\varphi)\sin\theta d\theta d\varphi, \tag{26}$$

$$F_{nm}^{H} = \frac{1}{\epsilon_{nm}} \int_0^{2\pi} \int_0^{\pi} \mathbf{f}_{nm}(R,\theta,\varphi)\mathbf{N}_{nm}^{t}(\theta,\varphi)\sin\theta d\theta d\varphi, \tag{27}$$

where:

$$\epsilon_{nm} = (-1)^m \frac{4\pi n(n+1)}{2n+1} \tag{28}$$

and $F_{nm}^{E} = \left\{C_{nm}^{E}, D_{nm}^{E}\right\}$, $F_{nm}^{H} = \left\{C_{nm}^{H}, D_{nm}^{H}\right\}$ denotes the fields expansion coefficients, $\mathbf{f}_{nm} = \{\mathbf{E}_t, \mathbf{H}_t\}$ are vector functions describing the distribution of the field on the surface $\mathcal{S}$ in region I for assumed value m and $n \in \{m, \ldots, N\}$. In FDFD technique the electric and magnetic fields are displaced for a half of the cell. Hence, in order to find the tangential electric field components exactly at the same radius as magnetic ones we calculate them as an arithmetic mean of two neighbouring samples. Utilizing defined by (26) and (27) coefficients the impedance matrix can be determined as follows:

$$\mathbf{Z}_m = \begin{bmatrix} \mathbf{C}_m^{E(E_{b(M_t)})} & \mathbf{C}_m^{E(E_{b(N_t)})} \\ \mathbf{C}_m^{H(E_{b(M_t)})} & \mathbf{C}_m^{H(E_{b(N_t)})} \end{bmatrix} \begin{bmatrix} \mathbf{D}_m^{E(E_{b(M_t)})} & \mathbf{D}_m^{E(E_{b(N_t)})} \\ \mathbf{D}_m^{H(E_{b(M_t)})} & \mathbf{D}_m^{H(E_{b(N_t)})} \end{bmatrix}^{-1}. \tag{29}$$

In above relation matrices $\mathbf{C}_m^{E(E_{b(M_t)})}$ and $\mathbf{C}_m^{H(E_{b(M_t)})}$ contains the electric and magnetic field expansion coefficients at the surface $\mathcal{S}$ for the excitation $\mathbf{E}_{b(M_t)}$ defined by relation (24) and take the form:

$$\mathbf{C}_m^{(\cdot)} = \begin{bmatrix} C_{mmm}^{(\cdot)} & C_{mm(m+1)}^{(\cdot)} & \cdots & C_{mmN}^{(\cdot)} \\ C_{mNm}^{(\cdot)} & C_{m(m+1)(m+1)}^{(\cdot)} & \ddots & C_{m(m+1)N}^{(\cdot)} \\ \vdots & \vdots & \ddots & \vdots \\ C_{mNm}^{(\cdot)} & C_{mN(m+1)}^{(\cdot)} & \cdots & C_{mNN}^{(\cdot)} \end{bmatrix}. \tag{30}$$

All the other matrices from Equation (29) are defined analogously.

Finally, determining $\mathbf{Z}_m$-matrix for all eigenvalues $m = -M, \ldots, M$ we are obtaining the desired impedance matrix in the following form:

$$\mathbf{Z} = \begin{bmatrix} \mathbf{Z}_{-\mathbf{M}} & \mathbf{0} & \mathbf{0} \\ \mathbf{0} & \ddots & \mathbf{0} \\ \mathbf{0} & \mathbf{0} & \mathbf{Z}_{\mathbf{M}} \end{bmatrix}. \tag{31}$$

It can be found that $\mathbf{Z}_{-m}$ can be simply calculated based on the known $\mathbf{Z}_m$ defined for $m > 0$. Using the Maxwell Equations (15) and (16) and the property of associated Legendre polynomials [20]:

$$P_n^{-m}(\cos\theta) = (-1)^m \frac{(n-m)!}{(n+m)!} P_n^m(\cos\theta) \tag{32}$$

we are obtaining the following relation:

$$\mathbf{Z}_{-m} = \mathbf{U}_m^{-1} \mathbf{Z}_m \mathbf{U}_m, \tag{33}$$

where: $\mathbf{U}_m = \text{diag}\{-U_{mm}, \ldots, -U_{mN}, U_{mm}, \ldots, U_{mN}\}$ and $U_{mn} = \frac{(n-m)!}{(n+m)!}$.

2.2. Multiple Object Analysis

In the analysis of multiple object configurations the iterative scattering procedure (ISP) formulated in spherical coordinates is used [17]. In this procedure each scatterer is represented by **T**-matrix defined in previous section. In the ISP we assume that the incident field on a single post in Pth iteration is derived from the scattered field from the remaining posts in the previous iteration. At the end of the procedure the total electric and magnetic fields on surface S_c are obtained. Bearing in mind that the scattered field obtained during iteration process depends on the unknown coefficients of zero order incident field, the investigated configuration of posts can be described by total transmission matrix $\mathbf{T}_{total}$. In above procedure the fields between each scatterers are translated using additional theorem of vector spherical harmonics (VSH) [22]. In this relations the expansion coefficients are determined using recurrence relations, which evaluation is numerically inefficient and time consuming. In many cases the procedure can be speed-up just by using the nested iterative scattering procedure (NISP) [24]. In this approach, at first the effective objects are evaluated for smaller groups of objects. Next, the total transmission matrix is determined for the group of effective spheres defined in previous step.

2.3. Plane Wave Scattering

The proposed hybrid technique can be easily applied to the analysis of scattering phenomenon from arbitrary configuration of axially-symmetrical posts located in free space and illuminated with any incident field. Lets consider in this section the plane wave illumination of the investigated structure (see Fig. 4). In this case the total tangential components of the electric and magnetic fields in the outer region of surface $\mathcal{S}$ enclosing analyzed structure are defined by

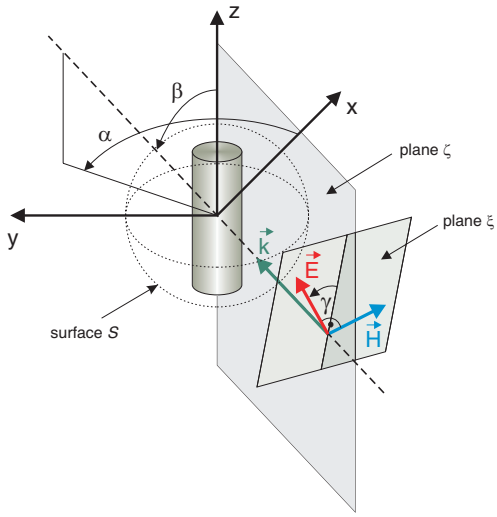

Figure 4. Plane wave in spherical coordinates.

Equations (2) and (3) where A^E_{1nm} and A^H_{1nm} are the coefficients of incident field:

$$A^E_{1nm} = \psi_{nm}\left\{\pi_{nm}(\beta)\cos\gamma + j\tau_{nm}(\beta)\sin\gamma\right\}, \tag{34}$$

$$A^H_{1nm} = \psi_{nm}\left\{\tau_{nm}(\beta)\cos\gamma + j\pi_{nm}(\beta)\sin\gamma\right\}, \tag{35}$$

and

$$\pi_{nm}(\beta) = \frac{\partial P^m_n(\cos\beta)}{\partial\beta}, \tag{36}$$

$$\tau_{nm}(\beta) = \frac{m}{\sin\beta}P^m_n(\cos\beta), \tag{37}$$

$$\psi_{nm} = E_0(-j)^n\frac{2n+1}{n(n+1)}e^{-jm\alpha}. \tag{38}$$

As a result of this excitation the scattered field with the unknown coefficients A_{2nm} is obtained. The coefficients of scattered field can be directly found from relation (6).

3. ACCURACY

The convergence of presented technique was verified for the single dielectric cylinder illuminated with plane wave (see Fig. 5). In the

analysis the following error criterion was assumed:

$$\delta_F = \frac{||F - F^{RE}||}{||F^{RE}||} \cdot 100\%, \quad \text{where:} \quad ||\cdot|| = \sqrt{\int_0^{2\pi}\int_0^{\pi} |\cdot|^2 d\theta d\varphi}, \quad (39)$$

F is a characteristic of scattered field pattern for assumed parameters of analysis and F^{RE} is a scattered field pattern obtained from Richardson extrapolation [25]. The results of convergence analysis are collected in Table 1. It can be noticed that the error becomes lower with the increasing mesh density W and the number of eigenfunctions N. For number of eigenfunctions $N = 6$ and mesh cells $W = 160 \times 240$ the accuracy of the method is higher than 0.1%. In this case the time of scattered field pattern computation is about 128 s. However, when we assume the accuracy higher than 0.6%, the satisfactory results are obtained for $W = 40 \times 60$ and $N = 6$. In this case, the time of calculation is about 2 s.

Table 1. Percentage error δ_F of scattered field pattern calculation for the structure from Fig. 5(a).

	Mesh density ($W = I \times K$)				
	10×15	20×30	40×60	80×120	160×240
$N = 2$	4.98	5.72	5.74	5.74	5.72
$N = 4$	2.74	1.23	0.59	0.24	0.11
$N = 6$	2.71	1.21	0.55	0.20	0.03
$N = 8$	2.71	1.23	0.58	0.24	0.05
$N = 10$	2.72	1.25	0.59	0.25	0.06

4. NUMERICAL RESULTS

In order to verify the validity and efficiency of the proposed approach three structures presented in Figs. 6–8 were analyzed.

The first investigated structure presented in Fig. 6 is a configuration of four dielectric cylinders illuminated with plane wave. The normalized scattered electric field pattern is presented in Figs. 6(b)–6(d). The results of proposed method well agree with the ones obtained from commercial software QuickWave 3D (FDTD). The computational time of hybrid FDFD-MM technique with $N = 8$ and $W = 20 \times 30$ cells is 6.1 s (0.7 s for single object transmission matrix) whereas the FDTD simulation with 546000 cells requires about 63 s

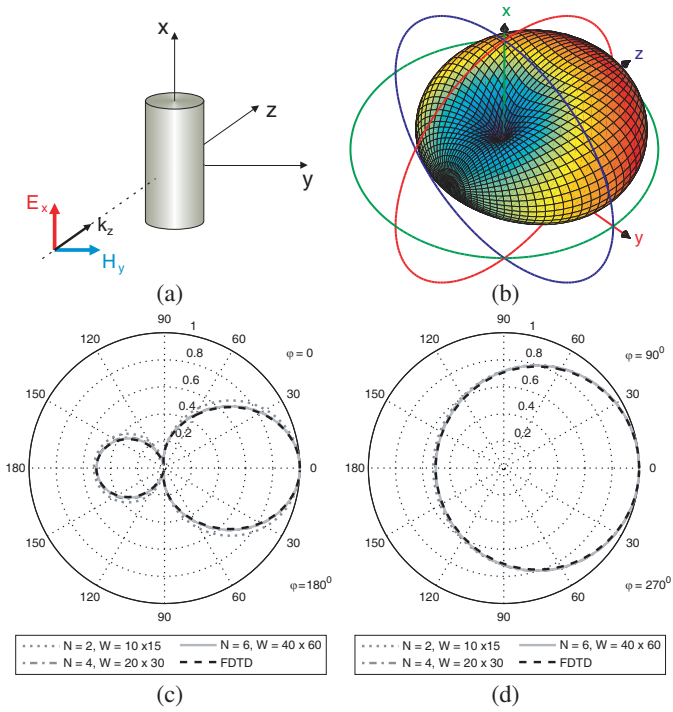

Figure 5. Plane wave scattering on single dielectric cylinder ($\varepsilon_r = 3$, $r = 6\,\text{mm}$, $h = 20\,\text{mm}$, $f_0 = 8\,\text{GHz}$): (a) investigated structure, (b) normalized scattered electric field pattern and its cross-sections in, (c) x-z-plane and (d) y-z-plane.

(about eleven times longer). From the presented results it can be also noticed that the usage of the investigated dielectric posts allows to obtain the directional scattered field pattern with the low level of side lobes. This property of dielectric objects can be applied in an antenna beam focusing systems.

The next structure presented in Fig. 7 is an array of four dielectric cylinders illuminated with plane wave. The scattered field patterns for different angles (according to the direction of plane wave incidence) of post configuration are presented in Figs. 7(a)–7(c). The results are compared with the ones obtained from FDTD technique and a good agreement is observed. In the case of hybrid approach with $N = 8$ and $W = 20 \times 30$ the time of calculations is about 11.2 s (0.7 s for single object transmission matrix) whereas the FDTD simulation with 312228 cells needs 87 s (about eight times longer). From the presented results it can be also noticed that the rotation of the posts has significant

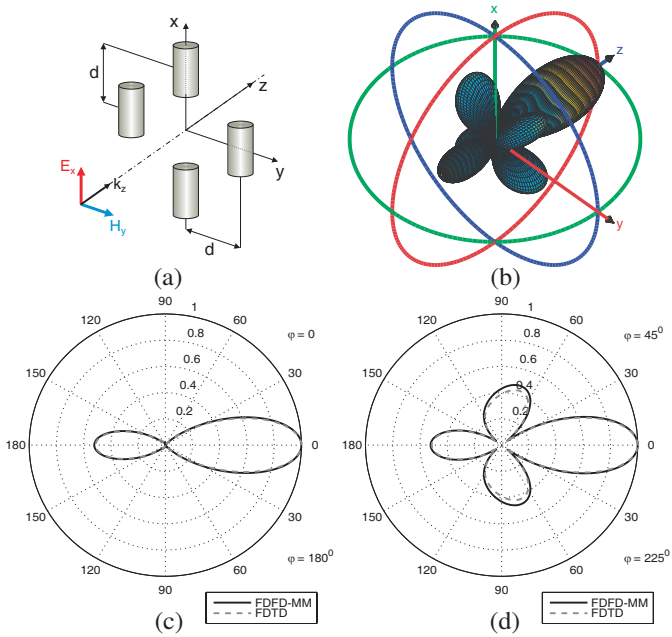

Figure 6. Plane wave scattering on configuration of four dielectric cylinders: (a) investigated structure ($r = 3\,\text{mm}$, $h = 10\,\text{mm}$, $d = 12\,\text{mm}$, $\varepsilon_r = 5$, $f_0 = 14\,\text{GHz}$), (b) normalized scattered electric field pattern and its cross-sections in (c) $\varphi = \{0, 180^\circ\}$ and (d) $\varphi = \{45^\circ, 225^\circ\}$ planes.

influence on the shape of scattered field pattern. This can be used in the beam forming structures.

The third structure is an array of sixteen metallic cylinders presented in Fig. 8(a). As in the previous case the analyzed set of objects is illuminated with plane wave. The normalized energy characteristics of scattered field pattern for two different frequencies of analysis are presented in Figs. 8(b) and 8(c). As in the previous cases results well agree with FDTD calculations. The computational time of the proposed method with $N = 8$ and $W = 2400$ is 34.2 s whereas the FDTD simulation with 2395600 cells requires 334 s (ten times longer). It can be also noticed that the periodically situated posts allows to transmit or reflect almost all the power of the incident wave for different frequencies. This effect can be used in periodic structures to obtain the frequency selective surfaces which has a wide range of applications in novel microwave systems.

The proposed hybrid technique is about ten times faster than commercial software. Moreover, the time of analysis of single post

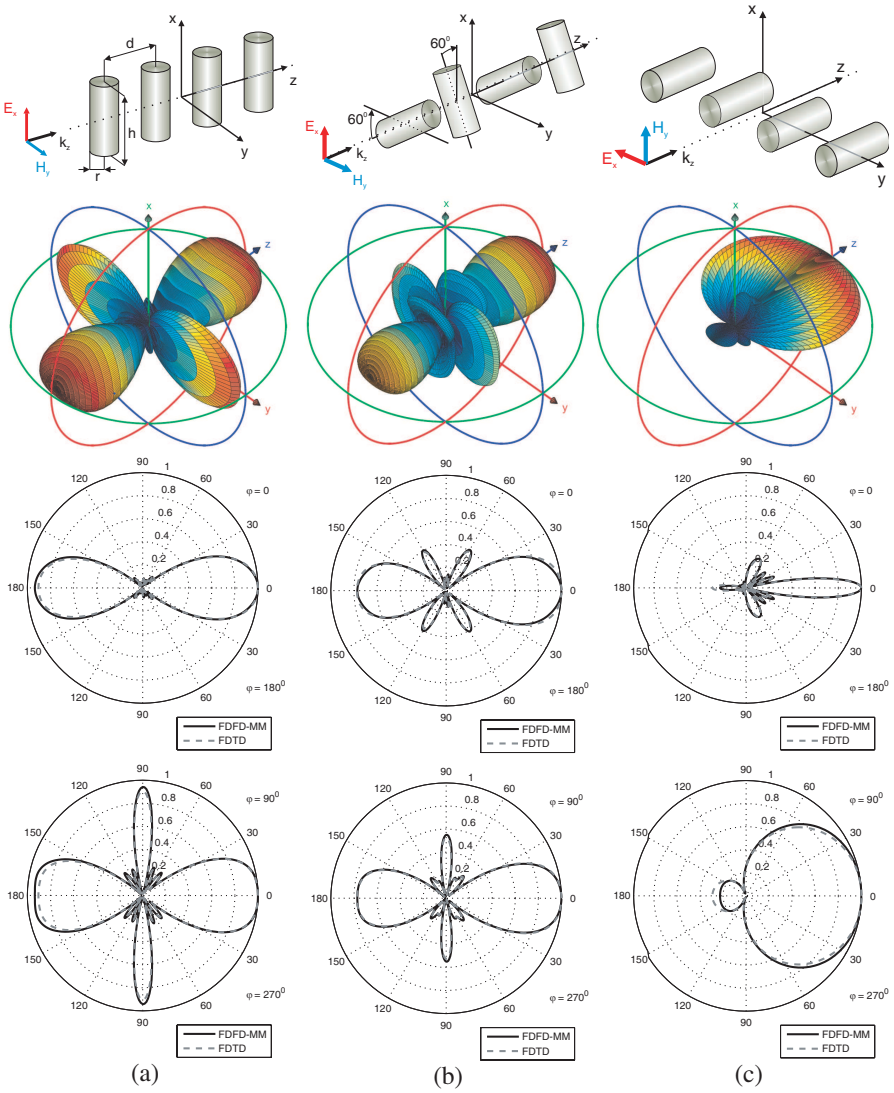

Figure 7. Plane wave scattering on configuration of four dielectric cylinders ($\varepsilon_r = 5$, $r = 3\,\text{mm}$, $h = 20\,\text{mm}$, $d = 30\,\text{mm}$, $f_0 = 10\,\text{GHz}$) for three different situations of posts according to plane wave incidence.

takes about only 10% of the whole time of analysis. The rest of the time is used in ISP to determine the scattering parameters of the investigated configuration. Most of the time in ISP is used to determine (from recurrence relations [22]) the series coefficients

describing the transformations of vector spherical harmonics between local coordinates. These relations are much simpler in the case of post rotation. It means that when the transmission matrix of each single post and all the transformation of fields in ISP between local

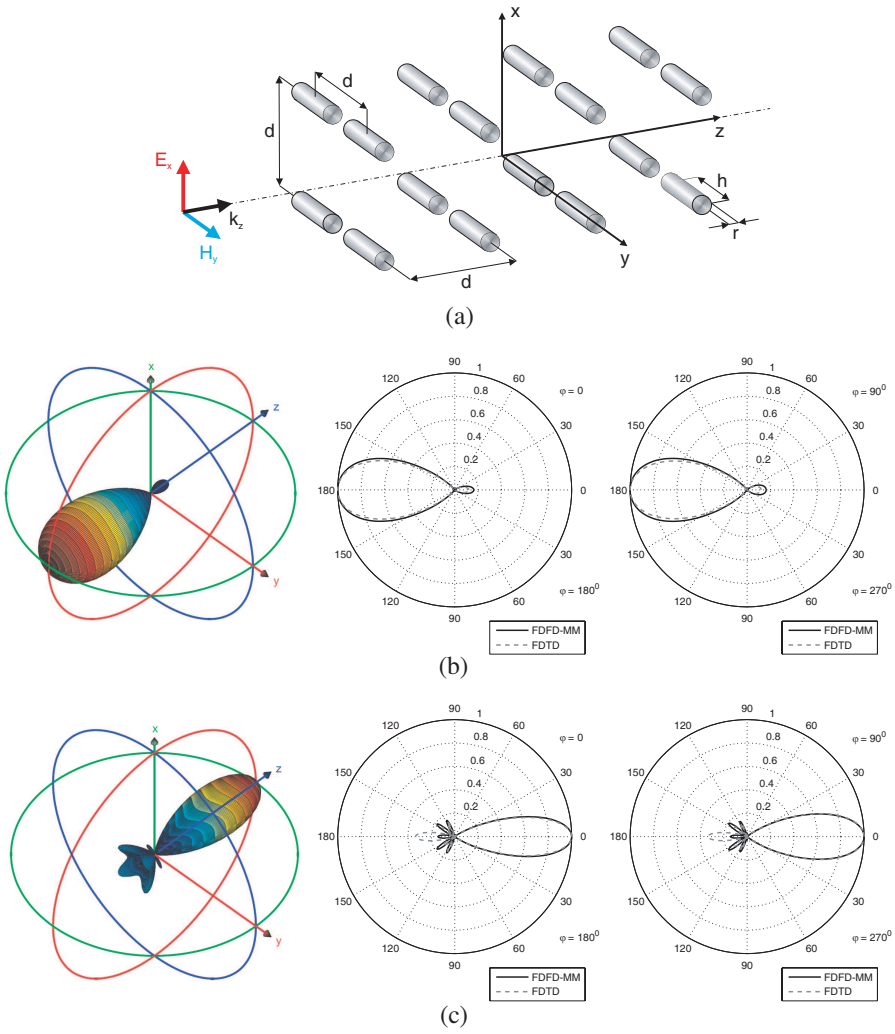

Figure 8. Plane wave scattering by an array of sixteen metallic cylinders ($r = 2\,\text{mm}$, $h = 18\,\text{mm}$, $d = 16\,\text{mm}$): (a) investigated structure and normalized scattered power pattern and its cross-sections for (b) $f_0 = 5\,\text{GHz}$, and (c) $f_0 = 6\,\text{GHz}$.

coordinates are determined once for desired frequency, the calculation time of scattering parameters of the structure for any angles of posts rotation is very short (about 0.1 s for all the investigated structures). In result this method becomes very efficient when the parameters of considered posts configuration for different rotation angles of elements has to be found.

5. CONCLUSION

In this paper the new hybrid method based on the combination of FDFD/MM technique and analytical ISP procedure is presented. The proposed approach is applied to the analysis of electromagnetic wave scattering from arbitrary configuration of objects. The convergence and efficiency of the method are examined. The numerical results are verified with commercial software and a good agreement is observed. For all the presented examples the proposed technique was about ten times faster in comparison to FDTD technique. Moreover, this method becomes very efficient, when the parameters of the structure for different angles of post rotation has to be found. This can be done just by use of presented in the paper simple analytical relation.

ACKNOWLEDGMENT

This work was supported in part by the Foundation for Polish Science under the Domestic Grants for Young Scientists Scheme, in part by the Polish State Committee for Scientific Research under Contract N515 346536 and in part by the Polish Ministry of Science and Higher Education from sources for science in the years 2010-2012 under COST Action IC0803, decision No 618/N-COST/09/2010/0.

APPENDIX A.

In Equations (10) and (11) matrices $\mathbf{M}_{A1}^{E}$, $\mathbf{M}_{A1}^{H}$, $\mathbf{M}_{A2}^{E}$ and $\mathbf{M}_{A2}^{H}$ take the following form:

$$\mathbf{M}_{(\cdot)}^{E} = \mathrm{diag}\left\{\mathbf{Z}_0, \mathbf{Z}_1, \ldots, \mathbf{Z}_N, \mathbf{dZ}_0, \mathbf{dZ}_1, \ldots, \mathbf{dZ}_N\right\}, \tag{A1}$$

$$\mathbf{M}_{(\cdot)}^{H} = \mathrm{diag}\left\{\mathbf{dZ}_0, \mathbf{dZ}_1, \ldots, \mathbf{dZ}_N, \mathbf{Z}_0, \mathbf{Z}_1, \ldots, \mathbf{Z}_N\right\}, \tag{A2}$$

where $\mathbf{Z}_n = z_n(k_2R)\mathbf{I}_{2n+1\times 2n+1}$, $\mathbf{dZ}_n = \frac{k}{j\omega\mu} z_n'(k_2R)\mathbf{I}_{2n+1\times 2n+1}$, $z_n'(\alpha x) = \frac{1}{\alpha x}\frac{\partial \alpha z_n(\alpha x)}{\partial x}$ and $\mathbf{I}_{2n+1\times 2n+1}$ is a unit matrix of dimension $2n+1 \times 2n+1$. In the case of matrice $\mathbf{M}_{A1}^{E,H}$ function $z_n(\cdot) = j_n(\cdot)$ and in the case of matrice $\mathbf{M}_{A2}^{E,H}$ function $z_n(\cdot) = h_n^{(2)}(\cdot)$.

REFERENCES

1. Ghaffar, A. and Q. A. Naqvi, "Focusing of electromagnetic plane wave into uniaxial crystal by a three dimensional plano convex lens," *Progress In Electromagnetics Research*, Vol. 83, 25–42, 2008.
2. Andres-Garcia, B., L. E. Garcia Munoz, V. Gonzalez-Posadas, F. J. Herraiz-Martnez, and D. Segovia-Vargas, "Filtering lens structure based on srrs in the low THz band," *Progress In Electromagnetics Research*, Vol. 93, 71–90, 2009.
3. Chien, W., "Inverse scattering of an un-uniform conductivity scatterer buried in a three-layer structure," *Progress In Electromagnetics Research*, Vol. 82, 1–18, 2008.
4. Solimene, R., A. Brancaccio, R. Pierri, and F. Soldovieri, "TWI experimental results by a linear inverse scattering approach," *Progress In Electromagnetics Research*, Vol. 91, 259–272, 2009.
5. Poli, L. and P. Rocca, "Exploitation of TE-TM scattering data for microwave imaging through the multi-scaling reconstruction strategy," *Progress In Electromagnetics Research*, Vol. 99, 245–290, 2009.
6. Andreasen, M., "Scattering from bodies of revolution," *IEEE Transactions on Antennas and Propagation*, Vol. 13, No. 2, 303–310, Mar. 1965.
7. Glisson, A. W. and D. R. Wilton, "Simple and efficient numerical techniques for treating bodies of revolution," *Tech. Rep.*, Vol. 22, University of Mississippi, Mar. 1979.
8. Huddleston, P. L., L. N. Medgyesi-Mitschang, and J. M. Putnam, "Combined field integral equation formulation for scattering by dielectrically coated conducting bodies," *IEEE Transactions on Antennas and Propagation*, Vol. 34, No. 4, 510–520, Apr. 1986.
9. Wu, T. K. and L. L. Tsai, "Scattering from arbitrarily-shaped lossy dielectric bodies of revolution," *Radio Sci.*, Vol. 12, No. 5, 709–718, 1977.
10. Medgyesi-Mitschang, L. N. and J. M. Putnam, "Electromagnetic scattering from axially inhomogeneous bodies of revolution," *IEEE Transactions on Antennas and Propagation*, Vol. 32, No. 8, 275–285, 1984.
11. Morgan, M. and K. Mei, "Finite-element computation of scattering by inhomogeneous penetrable bodies of revolution," *IEEE Transactions on Antennas and Propagation*, Vol. 27, No. 2, 202–214, Mar. 1979.
12. Greenwood, A. D. and J.-M. Jin, "Finite-element analysis of complex axisymmetric radiating structures," *IEEE Transactions*

on Antennas and Propagation, Vol. 47, No. 8, 1260–1266, Aug. 1999.

13. Jin, J.-M., "A highly robust and versatile finite element boundary integral hybrid code for scattering by bor objects," *IEEE Transactions on Antennas and Propagation*, Vol. 53, No. 7, 2274–2281, Jul. 2005.
14. Dunn, E. A., J.-K. Byun, E. D. Branch, and J.-M. Jin, "Numerical simulation of BOR scattering and radiation using a higher order FEM," *IEEE Transactions on Antennas and Propagation*, Vol. 54, No. 3, 945–952, Mar. 2006.
15. Yan, W.-Z., Y. Du, H. Wu, D. W. Liu, and B. I. Wu, "Emscattering from a long dielectric circular cylinder," *Progress In Electromagnetics Research*, Vol. 85, 39–67, 2008.
16. Yan, W.-Z., Y. Du, Z. Y. Li, E. X. Chen, and J. C. Shi, "Characterization of the validity region of the extended T-matrix method for scattering from dielectric cylinders with finite length," *Progress In Electromagnetics Research*, Vol. 96, 309–328, 2009.
17. Hamid, A.-K., I. R. Ciric, and M. Hamid, "Iterative solution of the scattering by an arbitrary configuration of conducting or dielectric spheres," *IEE Proceedings H Microwaves, Antennas and Propagation*, Vol. 138, No. 6, 565–572, Dec. 1991.
18. Kusiek, A. and J. Mazur, "Analysis of scattering from arbitrary configuration of cylindrical objects using hybrid finite-difference mode-matching method," *Progress In Electromagnetics Research*, Vol. 97, 105–127, 2009.
19. Quick Wave 3D (QWED), http://www.qwed.com.pl/.
20. Stratton, J. A., *Electromagnetic Theory*, Wiley, 2007.
21. Tsang, L., J. A. Kong, and K.-H. Ding, *Scattering of Electromagnetic Waves: Theories and Applications*, John Wiley and Sons, INC., New York, 2000.
22. Mackowski, D. W., "Analysis of radiative scattering for multiple sphere configurations," *Proceedings of the Royal Society, Series A — Mathematical and Physical Sciences*, Vol. 433, No. 1889, 599–614, Jun. 1991.
23. Taflove, A., *The Finite-difference Time-domain Method*, Artech House, 1995.
24. Polewski, M. and J. Mazur, "Scattering by an array of conducting lossy dielectric, ferrite and pseudochiral cylinders," *Progress In Electromagnetics Research*, Vol. 38, 283–310, May 2002.
25. Dahlquist, G. and A. Bjorck, *Numerical Methods*, Prentice Hall, 1974.